Zbigniew RYMARSKI, Krzysztof BERNACKI

Silesia University of Technology, Institute of Electronics

The influence of the output impedance of the DC voltage source on the dynamic properties of the voltage source inverter for UPS system

Abstract. *In many cases, the voltage source inverter in a UPS system requires increasing its input DC voltage. Regardless of the specific solution, a DC/DC converter that stores energy in the inductance is usually applied. That is why it should be expected that this inductance multiplied by the square of the voltage increasing factor in connection with the DC/DC converter output capacitor will consist of the equivalent circuit on the inverter input. The aim of the paper is to demonstrate the impact of such equivalent impedance on the dynamic properties of the inverter. The investigation of the developed inverter model will allow the question of whether the choice of the appropriate feedback compensating the effects of the additional resonant frequencies in the magnitude frequency domain that are characteristic of the control function is necessary depending on DC/DC converter parameters to be answered. The paper shows both software simulations and experimental laboratory model measurements.*

Streszczenie. *W wielu wypadkach należy podwyższyć napięcie wejściowe inwertera pracującego w systemie UPS. Bez względu na specyficzne rozwiązanie zwykle stosowane są przetwornice napięcia stałego gromadzące energię w indukcyjności. Dlatego należy oczekiwać że ta indukcyjność pomnożona przez kwadrat współczynnika podwyższania napięcia, w połączeniu z wyjściowym kondensatorem przetwornicy DC/DC będzie stanowić zastępczą impedancję na wejściu inwertera. Celem artykułu jest pokazanie wpływu takiej zastępczej impedancji na własności dynamiczne inwertera. Badanie zmodyfikowanego modelu inwertera pozwoli odpowiedzieć na pytanie, czy jest konieczny dobór odpowiedniego sprzężenia zwrotnego kompensującego zmiany charakterystyki amplitudowo-częstotliwościowej spowodowane dwoma dodatkowymi częstotliwościami rezonansowymi, zależnie od parametrów przetwornicy DC/DC. Artykuł przedstawia zarówno symulacje programowe jak i pomiary eksperymentalnego modelu laboratoryjnego* ***(Wpływ wyjściowej impedancji źródła napięcia stałego na własności dynamiczne inwertera napięcia przeznaczonego do systemu UPS).***

Keywords: output impedance, PWM, Bode plots (frequency domain characteristics).
Słowa kluczowe: impedancja wyjściowa, modulacja PWM, charakterystyki częstotliwościowe.

Introduction

Standard UPS voltage source inverters (VSI) should have an output rms voltage of 230 V. Serially connected batteries in inverters without an output transformer can be used to get a high enough DC voltage. However, for the low output power of the inverter, this is an ineffective solution financially. An output transformer that increases the voltage can be used together with inexpensive low voltage batteries. However, in this case the whole inverter device works in the primary transformer side and all its parasitic resistances are transformed with the square of the transformer turn ratio to the output [1]. The possibility of the magnetic saturation of the transformer core caused by the asymmetry of the magnetizing current is a serious problem. The other solution is to use a DC/DC converter to increase the input DC voltage. For the last 10 years, the solution has been a Z-Source impedance network that uses the additional states of the single- or 3-phase bridge inverter switches [2]. There are many improved Z-Source versions, e.g. LCCT qZSI (inductor-capacitor-capacitor-transformer quasi Z-Source inverter) presented in [3], which has an almost constant input current (the discontinuous current from DC source was one of the disadvantages of the basic Z-Source) owing to an additional inductor serially connected with the input switching diode. The detailed design does not matter because all of DC/DC converters that increase the input voltage store energy in the inductances, which influences the inverter output voltage distortions for the standard types of loads. The output equivalent inductance L_{CONe} of the DC/DC converter is the function of storing energy inductance L_{DC} multiplied by the square of the DC voltage increasing factor k_V (Fig. 1). This equivalent inductance L_{CONe} is connected with the DC/DC converter output equivalent capacitance C_{CONe} (in most cases it is simply equal to C_{CON} – converter output capacitor). The novelty of the solution presented in this paper is the implementation of the output equivalent impedance to a small signal model of a single-phase H-bridge, 3-level voltage source inverter. This model is useful to answer the question of whether the design of the control loop that will correct the Bode characteristics of the control function that compensate the effects of the additional resonant frequencies introduced by the DC/DC converter storage inductor is necessary for the particular case of the converter parameters set. It should be noted that these resonant frequencies are much lower than the resonant frequency of the inverter output filter, which is always designed below half of the switching frequency. This means that it is possible to effectively remove their impact from the closed loop system characteristics by using an efficient controller. The problems of stability DC/AC and DC/DC converters have considerable impact on their design and are widely presented in the literature [4].

The design of the voltage source inverter should always start with the design of the output L_FC_F filter and the choice of the PWM type and scheme [5], [6]. The other problem of inverter design is taking the influence of the PWM scheme on the electromagnetic compatibility of the whole inverter and its radiators acting as unintentional antennas into consideration [7], [8]. Creating the “cost function” of the reactive power in the filter components and the assumption that the reactive power of an inductor is weighted two times higher than that of the capacitor was the most popular approach of the design of an L_FC_F filter [9], [10], [11] although it was not justified. In this paper the design of the filter presented in [12] was based on [13] where the minimization of the reactive power in the filter components without additional weights is used. This paper concerns the simplest case of a single-phase, H-bridge, 3-level inverter. The L_F and C_F values [5], [6], [12] depend on the load ($V_{IOUTrms}$ – the VSI output rms voltage, $I_{IOUTrms}$ the VSI output rms current) and the switching frequency f_c.

$$(1) \qquad L_F \approx \frac{1}{f_c}\frac{V_{IOUTrms}}{I_{IOUTrms}},\ C_F \approx \frac{1}{f_c}\frac{1}{V_{IOUTrms}/I_{IOUTrms}}$$

Inverter model

The averaged in the switching period the voltage source inverter model with the load current as an independent disturbance (e.g. [9], [14]) has been widely presented. This approach requires the careful analysis of the influence of

load changes on the stability of the closed loop system for the chosen controller [15]. The output impedance of the DC/DC converter circuit (Fig. 1) should be included (Fig. 2) in the model because its impact on the control function of the inverter is noticeable, which will be shown in this paper. The inverter filter parameters were calculated from (1). The PWM modulator transfer function is assumed $H_{PWM}(s)=1$ [9], [10]. The load resistance R_0 strongly damps some of the resonant effects in the control transfer function and is included in the final equations (4).

The control transfer function $K_v(s)=V_{IOUT}/V_{CTRL}$ (Fig. 2) is described by (2).

$$K_v(s)=\frac{V_{IOUT}(s)}{V_{CTRL}(s)}=\frac{N(s)}{D(s)}=$$

$$(2)\qquad =\frac{\omega_{F0}{}^2(s^2+s\frac{R_{CONe}}{L_{CONe}}+\omega_{CONe}{}^2)}{s^4+b_3s^3+b_2s^2+b_1s+(1+\frac{R_{CONe}+R_{LF}}{R_O})\omega_{F0}{}^2\omega_{CONe}{}^2}$$

where $\omega_{CONe}{}^2=1/(L_{CONe}C_{CONe})$, $\omega_{FO}{}^2=1/(L_FC_F)$

$$b_3=\frac{R_{CONe}}{L_{CONe}}+\frac{R_{LF}}{L_F}+\frac{1}{R_OC_F}$$

$$b_2=\omega_{CONe}{}^2+\frac{R_{CONe}}{L_{CONe}}(\frac{R_{LF}}{L_F}+\frac{1}{R_OC_F})+$$

$$+\omega_{FO}{}^2(1+\frac{R_{LF}}{R_0}+\frac{C_F}{C_{CONe}})$$

$$b_1=\omega_{CONe}{}^2(\frac{R_{CONe}+R_{LF}}{L_F}+\frac{1}{R_OC_F})+$$

$$+\omega_{FO}{}^2[(1+\frac{R_{LF}}{R_O})\frac{R_{CONe}}{L_{CONe}}+\frac{1}{R_OC_{CONe}}]$$

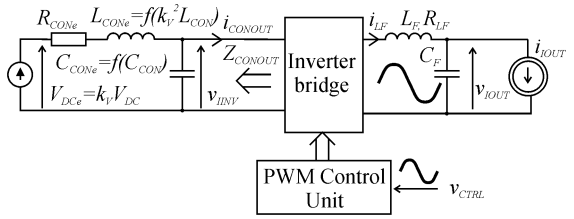

Fig. 1. VSI with the equivalent circuit of the DC/DC converter increasing the input DC voltage

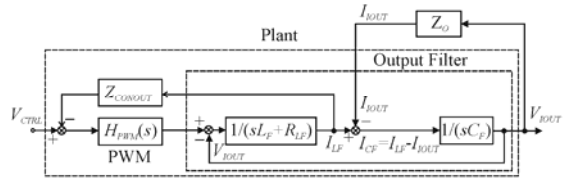

Fig. 2. Simple averaged inverter model including the DC/DC converter output impedance Z_{CONOUT}

In the standard inverter design ($C_{CONe}>>C_F$), the function $K_v(s)$ (2) can be approximated by equation (3) where $K_{v0}(s)$ (4a) is the control transfer function of the inverter without the DC/DC converter. The roots of nominator and denominator of the $K_{CON}(s)$ function from (4b) are very closely placed on the frequency axis. Bode frequency domain characteristics (3) nearly cover (2) for a wide spectrum of inverter and converter parameters. The presented $K_{CON}(s)$ function (4b) is highly dependent on the damping factors that are different in the nominator and denominator. It is not possible to skip the load resistance R_O that is connected parallel to C_F (as in assumptions of the inverter model) because it has a considerable influence on the damping factor of the denominator.

$$(3)\qquad K_v(s)\approx K_{v0}(s)K_{CON}(s)$$

where

$$(4a)\quad K_{v0}(s)=\frac{\omega_{F0}{}^2}{s^2+s(\frac{R_{LF}}{L_F}+\frac{1}{R_OC_F})+(1+\frac{R_{LF}}{R_O})\omega_{F0}{}^2}$$

(4b)

$$K_{CON}(s)=\frac{s^2+sk_N\frac{R_{CONe}}{L_{CONe}}+\omega_{CONe}{}^2}{s^2+sk_D(\frac{R_{CONe}}{L_{CONe}}+\frac{1}{R_OC_{CONe}})+\omega_{CONe}{}^2(1+\frac{R_{CONe}}{R_O})}$$

The approximated formula (5) of the inverter output impedance Z_{IOUT} can be presented where Z_{IOUT0} is the inverter output impedance without the DC/DC converter.

$$(5)\qquad Z_{IOUT}(s)\approx K_v(s)[sL_F+\alpha(s)],$$

where

$$\alpha(s)\approx sL_{CONe}\frac{\omega_{CONe}{}^2}{s^2+\omega_{CONe}{}^2}$$

The input DC/DC converter components increases output impedance. It should be noted from (3), (4) and (5) that the DC/DC converter introduces 2 additional resonant frequencies to the inverter control function and to its output impedance. The additional, damping correcting coefficients k_N and k_D are implemented in order to make magnitude plots in the theoretical and the measured plot approximately equal because the close neighborhood of the resonant frequencies in the nominator and denominator of (4b) means that the function $|K_{CON}(\omega)|$ is very sensitive for damping serial resistances that can never be precisely calculated.

An analysis of Fig. 3 (L_{CONe}=1.5 mH, C_{CONe}=100 µF, L_F=0.5 mH, C_F=1 µF, f_c=25600 Hz, R_{CONe}=1.3 Ω, R_{LF}=0.1 Ω, R_O=100 Ω) indicates that the DC/DC converter has an influence on the dynamic properties of the VSI. The value of the DC/DC converter inductance should be decreased to lower this impact, but the converted energy should be stored in it. The solution is to increase the switching frequency of the DC/DC converter. An effective feedback loop is able to reduce the impact of a DC/DC converter. The presented simulation shows the case without the correcting coefficients (both equal to 1).

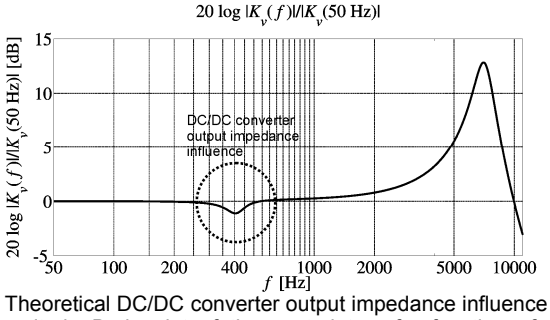

Fig. 3. Theoretical DC/DC converter output impedance influence on the magnitude Bode plot of the control transfer function of the voltage source inverter (L_{CONe}=1.5 mH, C_{CONe}=100 µF, L_F=0.5 mH, C_F=1 µF, f_c=25600 Hz, R_{CONe}=1.3 Ω, R_{LF}=0.1 Ω, R_O=100 Ω, k_N=1, k_D=1)

The influence of the DC/DC converter output is important only in the restricted frequency range and it does not visibly change all of the magnitude frequency domain characteristics. In a real inverter, the resonance peaks in

the magnitude plot will be seriously damped by means of the load resistance and it can be expected that these resonances can be important for harmonic disturbances, e.g. for the nonlinear rectifier RC load.

In many previous papers (e.g. [1], [5], [16], [17], [18]), it was shown that a reduction of the output voltage distortions for a nonlinear load (rectifier with RC load and the power factor 0.7) defined in EN-62040 requires an MISO control (with the controller inputs: the output voltage, the load current, the filter inductor current) or a multi-loop SISO control, e.g. with a CDM (Coefficient Diagram Method) controller [19], [20] in the inner loop and a repetitive controller in the outer loop. The solution with a repetitive controller is simple (it does not require current sensing) and robust for the load changes.

The CDM is a pole placement-polynomial approach method of a control. It places the poles of the closed loop system by means of the choice of its characteristic equation coefficients, which are dependent on the assigned time constant τ of the closed loop system. This constant τ influences the stability and robustness of the system and it was shown [15] that $\tau \approx 3T_c$ is a proper choice for the VSI to have a robust control system (for changes of the filter parameters and the load). The degrees of the $K(s)$ nominator and $L(s)$ denominator of the controller $K_{CTRL}(s)=K(s)/L(s)$ should be equal to or greater than the degree of denominator $D(s)$ of the plant transfer function in case of disturbances, e.g. the load current [21]. It was set at the 4-th degree of $K(s)$ and $L(s)$. Only this degree provides the robustness for disturbances while the load current is treated as a disturbance [14]. For a lower degree of the nominator and denominator of the CDM controller, additional resonant frequencies will still be visible for low damping resistances in the Bode plots of the inverter control function.

Experimental verification

The control voltage $v_{CTRL}(k)$ (6a), (6b) is the inverter sinusoidal reference voltage $v_{ref}(k)$ where $k=1\div512$ ($f_c=512f_m$). The fundamental waveform (f_m) has been summed with the excitation n-th harmonic (nf_m) sinusoidal waveforms (amplitudes of n-th harmonics were set to 0.2 of the fundamental harmonic amplitude). A double-edge 3-level modulation was used, so for a PWM Timer clock equal to 60 MHz (LPC2148, ARM7 microprocessor) and f_c=25600 Hz, the maximum amplitude was 1171 [22], M was equal to 0.8.

(6a)

$$v_{CTRL}(k)\big|_n = v_{ref}(k)\big|_n =$$

$$= round\left(A\{0.8\sin[(k-1)\frac{2pi}{512}] + 0.2\sin[n(k-1)\frac{2pi}{512}]\}\right)$$

(6b) $$if\ v_{CTRL}(k)\big|_n < 0\ then\ v_{CTRL}(k)\big|_n = 0$$

Where the really forced in the microprocessor based controller, absolute amplitude is:

$$A = M\frac{PWM\ Timer\ clock}{2f_c}$$

But for the modeling purpose, for the assumption $HPWM(s)=1$, it was used $A=MV_{CONOUTmax}$ (in Fig 2). All the transfer control function calculations concern relative values (7) where A disappears.

$$(7)\quad \left|K_{v\log}(n\omega_m)\right| = 20\log\frac{V_{hn}(n\omega_m)/V_{fm}(\omega_m)}{V_{ref-hn}(n\omega_m)/V_{ref-fm}(\omega_m)}$$

Where $V_{hn}(n\omega_m)$ is the amplitude of the inverter output voltage n-th harmonic $n\omega_m$, $V_{fm}(\omega_m)$ is the amplitude of the inverter output voltage fundamental harmonic ω_m for the particular stimulation (the example: Fig. 4a presents the stimulation for the 6-th harmonic, Fig. 4b presents the inverter output voltage for this stimulation). The denominator of (7): $V_{ref-hn}(n\omega_m)/V_{ref-fm}(\omega_m)$ is the ratio of the amplitude of the stimulated n-th harmonic and the amplitude of the fundamental harmonic of the reference waveform in this stimulation (it should be 0.25 ideally but it is a bit different). These ratios for the used stimulations waveforms are initially calculated and presented in Fig. 5b. For the even harmonics of f_m=50 Hz for $f_{hn\_even}/f_m \geq 6$ ($f_{hn\_even} \geq 300$ Hz) and for odd harmonics when n≥19 the waveform (6a) for the first half of the fundamental period it is negative in the short term and in the second half period it is positive in the short term. There is no possibility to generate the two different polarizations of the output voltage in one half of the fundamental period in the modulation scheme for 3-level PWM used so (6b) should be calculated.

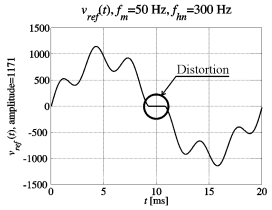

a) The reference voltage (6) for n=6

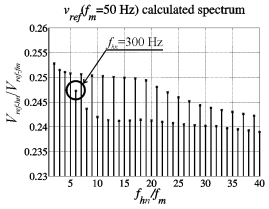

b) $V_{ref-hn}(n\omega_m)/V_{ref-fm}(\omega_m)$

Fig. 4. a) The stimulated data; b) the stimulated harmonics relative amplitudes b)

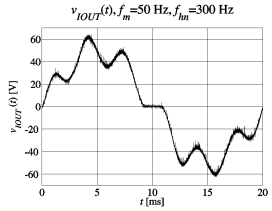

a) The measured output data for n=6

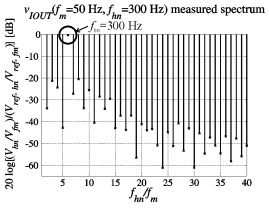

b) The spectrum of the waveform from a) after calculation (7)

Fig. 5. a) The measured data; b) the calculated spectrum for n=6

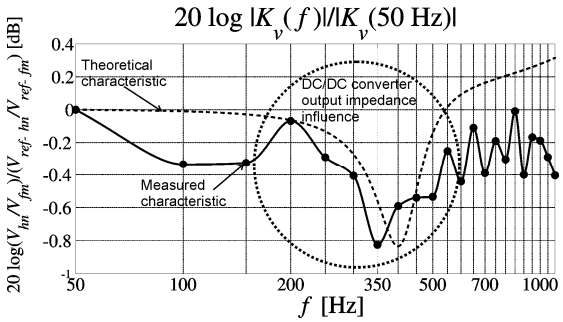

Fig. 6. Theoretical plot a) and measurements b) of the Bode plot of the control transfer function of the voltage source inverter (L_{CONe}=1.5 mH, C_{CONe}=100 μF, L_F=0.5 mH, C_F=1 μF, f_c=25600 Hz, R_{CONe}=1.3 Ω, R_{LF}=0.1 Ω, R_O=100 Ω, k_N=1, k_D=1)

The frequency range of excitation signals was chosen after theoretical analysis (Fig. 3) to show the influence of the converter impedance. The theoretical plot and results of measurements of the low power inverter (L_{CONe}=1.5 mH, C_{CONe}=100 μF, L_F=0.5 mH, C_F=1 μF, f_c=25600 Hz, R_{CONe}=1.3 Ω, R_{LF}=0.1 Ω, R_O=100 Ω, k_N=1, k_D=1) are presented in Fig. 6. The resolution of the presented analysis method is equal to f_m=50 Hz. The influence of a DC/DC converter on the control transfer function is highly dependent on damping parasitic resistances and the load resistance which can

significantly reduce this influence. Fig. 7 is an example of the measured influence of the Z-Source [2] increasing 5 times the maximum DC voltage (this is the reason of the high values of the equivalent parameters) and working in the Continuous Current Mode.

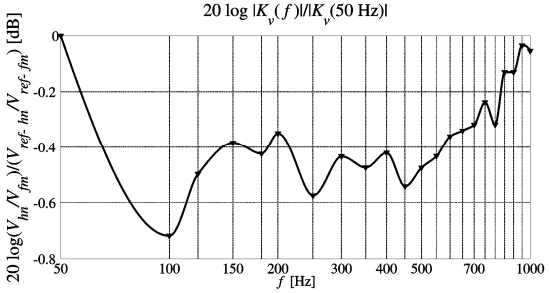

Fig. 7. Measurements of the Bode plot of the control transfer function of the voltage source inverter with Z-Source impedance network (L_{CONe}=35 mH, C_{CONe}=200 μF, L_F=2.2 mH, C_F=1 μF, f_c=25600 Hz, R_{CONe}=3 Ω, R_{LF}=0.1 Ω, R_O=94 Ω, Continuous Current Mode, the shoot-through time ratio d_Z=0.4)

Conclusions

The presented research shows the impact of the impedance of a DC/DC converter output on the control transfer function. The calculated and measured, using the laboratory inverter model, impact is highly dependent on the damping parasitic resistances and the load resistance. The measurements of the frequency dependent characteristics were limited to the f_m resolution of exciting frequencies, only harmonics of the fundamental frequency f_m were used, (Fig. 7 presents the expanded measurements for 120 Hz and 180 Hz), which could have a low influence on the identification of resonant frequencies. The presented model should enable the estimation if the design of the controller of the VSI takes the impact of the converter output impedance into consideration. This impact (mainly the effect of lowering magnitude) can be important for a nonlinear load that causes harmonic disturbances. The two additional resonant frequencies that are very close to each other in the control transient function can require a higher degree of the controller transfer function for low damping in the input inverter network. Further research should investigate the influence of specific DC/DC converter solutions, e.g. a Z-Source impedance network and the VSI control loop design for using this type of DC/DC converter. However in all the DC/DC converters increasing DC voltage their output equivalent resistance increases with the square of the voltage increasing factor what seriously increases the damping factor and the final influence of the converter output impedance on the control transfer function of the inverter is not so important as it could be expected (Fig. 7).

REFERENCES

[1] Rymarski Z., Amplitude Control In Single-Phase Inverters, *International Conference on Signals and Electronic Systems ICSES'06,* September 17-20, 2006, Łódź, Poland, pp. 331-334

[2] Peng F. Z., Z-Source Inverter, IEEE Transactions on Industry Applications, vol. 39, no. 2, March/April 2003, pp. 504 – 510, 2003

[3] Adamowicz M., Strzelecki R., Peng F., Guzinski J., Abu Rub H., New Type LCCT-Z-Source Inverters*, Proceedings of the 2011-14TH European Conference On Power Electronics And Applications* (EPE 2011) Birmingham, England, Aug 30-Sep 01, 2011

[4] Grzesik B., Sieweniak P., Lyapunov Stability Analysis of DC-DC Power Electronic Converters: A Brief Overview, *Przegląd Elektrotechniczny*, 88 (2012), No.9A, 162 – 166

[5] Rymarski Z., Complete design method of single-phase inverters for UPS systems, *International Journal of Electronics*, vol. 96, Issue 5, May 2009, pp. 521 – 535, 2009

[6] Rymarski Z., Zagadnienia projektowe jednofazowych inwerterów napięcia w układach UPS, *Elektronika - Konstrukcje, Technologie, Zastosowania*, SIGMA-NOT, No. 11/2007, pp. 367 - 372

[7] Bernacki K., Noga A., Analiza wpływu połączeń radiatora z płaszczyzną odniesienia na poziomy emisji promieniowanej, *Przegląd Elektrotechniczny*, R. 89 NR 4/2013, pp. 36 - 39

[8] Bernacki K., Noga A., Numerical and Experimental Analysis of Radiated Emissions from Different Heat Sink Configurations, *22nd International Conf. Radioelektronika 2012*, 17-18 April Brno, Czech Republic, pp. 40 - 42

[9] Kim J., Choi J., Hong H., Output LC filter design of voltage source inverter considering the performance of controller, *International Conference on Power System Technology*, PowerCon 2000, vol. 3, 4 - 7 Dec. 2000, pp. 1659 – 1664

[10] Ryu B., Kim J., Choi Ch., Design and analysis of output filter for 3-phase UPS inverter, *Power Conversion Conference*, 2 - 5 April 2002, vol. 3, pp. 941 – 946

[11] Dewan S. B., Ziogas P. D., Optimum Filter Design for a Single-Phase Solid-State UPS System, *IEEE Transactions on Industry Applications,* vol. IA-15, Issue 6, November/December 1979, pp. 664 – 669, 1979

[12] Rymarski Z., The discrete model of power stage of the voltage source inverter for UPS, *International Journal of Electronics*, vol. 98, No 10, October 2011, pp. 1291-1304

[13] Dahono P. A., Purwadi A., Qamaruzzaman, An LC filter design method for single-phase PWM inverters, *International Conference on Power Electronics and Drive System* 21 - 24 February 1995, vol. 2, pp. 571 – 576

[14] Kusko A., Galler D., Medora N., Output impedance of PWM UPS inverter-feedback vs. filters, *IEEE Industry Applications Society Annual Meeting*, 7 - 12 October 1990, vol. 2, pp. 1044 – 1048

[15] Rymarski Z., Wpływ tolerancji parametrów filtra wyjściowego i obciążenia na sterowanie PID/CDM jednofazowego inwertera napięcia, *Przegląd Elektrotechniczny*, 87 (2011), No.10, pp. 114-117

[16] Rymarski Z., The analysis of the output voltage distortions minimization in the 3-phase VSI for the nonlinear rectifier ROCO load, *Przegląd Elektrotechniczny*, 85 (2009), No.4, pp. 127 – 132

[17] Rymarski Z., Design method of a 3-phase VSI for UPS systems, *Conference: International Conference on Signals and Electronic Systems* (ICSES 2008) Location: Cracow, POLAND, Date: SEP 14-17, 2008, conference proceedings, pp. 293-296

[18] Rymarski Z., Control Systems of Single-Phase Voltage Source Inverters for a UPS, *Proceedings of 11-th IFAC/IEEE International Conference On Programmable Devices And Embedded Systems*, PDeS 2012, BRNO, May 23-th-25-th, 2012, pp. 291 - 296

[19] Manabe S., Coefficient Diagram Method, *14th IFAC Symposium on Automatic Control in Aerospace*, 1998, pp. 199 – 210

[20] Manabe S., Importance of coefficient diagram in polynomial method, *42nd IEEE Conference on Decision and Control*, vol. 4, 9 - 12 December 2003, pp. 3489 – 349

[21] Hamamci, S. E., Kaya, I., Koksal, M., Improving Performance For A Class of Processes Using Coefficient Diagram Method, *The 9th Mediterranean Conference on Control and Automation*, MED'01, Dubrovnik, Croatia, June 27 - 29, 2001

[22] Rymarski Z., Dobór mikrokontrolera do sterowania inwerterem napięcia w systemach UPS, *Elektronika - Konstrukcje, Technologie, Zastosowania*, SIGMA-NOT, No. 11/2012, pp. 111 - 114

***Authors**: dr hab. inż. Zbigniew Rymarski, Politechnika Śląska, Instytut Elektroniki, ul. Akademicka 16, 44-100 Gliwice, E-mail: zbigniew.rymarski@polsl.pl; mgr inż. Krzysztof Bernacki, Politechnika Śląska, Instytut Elektroniki, ul. Akademicka 16, 44-100 Gliwice, E-mail: krzysztof.bernacki@polsl.pl*